Journal of Marine Science and Technology

Volume 23 | Issue 4 Article 17

THE KRIGING CLOUD COMPUTING FRAMEWORK: INTERPOLATION OF TOPOGRAPHY BY CLOUD COMPUTING WITH THE KRIGING ALGORITHM

Cheng-Tsan Lai
Department of Harbor and River Engineering, National Taiwan Ocean University, Keelung, Taiwan

Sung-Shan Hsiao
Department of Harbor and River Engineering, National Taiwan Ocean University, Keelung, Taiwan, R.O.C

Hui-Ming Fang
Department of Harbor and River Engineering, National Taiwan Ocean University, Keelung, Taiwan, R.O.C

Edward H. Wang
Department of Civil Engineering and Environmental Informatics, Minghsin University of Science and Technology, Hsinchu, Taiwan, edwang313@gmail.com

Recommended Citation

Lai, Cheng-Tsan; Hsiao, Sung-Shan; Fang, Hui-Ming; and Wang, Edward H. (2015) "THE KRIGING CLOUD COMPUTING FRAMEWORK: INTERPOLATION OF TOPOGRAPHY BY CLOUD COMPUTING WITH THE KRIGING ALGORITHM," *Journal of Marine Science and Technology*: Vol. 23: Iss. 4, Article 17.
DOI: 10.6119/JMST-015-0512-1
Available at: https://jmstt.ntou.edu.tw/journal/vol23/iss4/17

THE KRIGING CLOUD COMPUTING FRAMEWORK: INTERPOLATION OF TOPOGRAPHY BY CLOUD COMPUTING WITH THE KRIGING ALGORITHM

Acknowledgements

This work was supported by the National Science Foundation in Taiwan, Grant No. NSC100-2221-E-019-010.The authors would like to thank all colleagues and students who contributed to this study.

Journal of Marine Science and Technology, Vol. 23, No. 4, pp. 534-540 (2015)
DOI: 10.6119/JMST-015-0512-1

THE KRIGING CLOUD COMPUTING FRAMEWORK: INTERPOLATION OF TOPOGRAPHY BY CLOUD COMPUTING WITH THE KRIGING ALGORITHM

Cheng-Tsan Lai[1], Sung-Shan Hsiao[1], Hui-Ming Fang[1], and Edward H. Wang[2]

Key words: topography, Kriging Modeling (KG), cloud computing.

ABSTRACT

Spatial information surveyed by photogrammetry, airborne LiDAR and Mobile Measurement System (MMS) above ground level can be analyzed by scientists using standard geostatistical methodologies such as ordinary Kriging and sequential Gaussian simulation to interpolate heterogeneities of profiles from sparse sample data. Proven effective by researchers, the Kriging algorithm model is used by commercial data analysis packages for instant interpolation. However, meaningful and reliable results only come with a comprehensive understanding of the variogram associated with valid mathematical functions. To capture spatial landscape variations from massive sample grids of satellite images, this paper presents a cloud computing-based automation approach to improve topography interpolation by taking advantage of rapid computation speed through an open-source cross platform to enrich internet applications. The research team conducted a pilot test on sand beaches, developed the Kriging Cloud Computing Framework, streamlined the Kriging algorithm, developed Kriging Variogram Data Bank and Parameter Management System, derived cross validation procedures and built in Application Programming Interface, API. This new technology can benefit end users around the world in acquiring of ground profiles and production of Digital Elevation Models (DEMs) while requiring only minimal knowledge of the Kriging Method. This cloud computing system facilitates user data input, parameter selection, fast data analysis and model output. The application of this new framework improves remote sensing technology and GIS applications in a variety of unreachable terrains, such as deserts, swamps, and dense forests.

I. INTRODUCTION

A proliferation of new topographic sensing technologies has complicated the interpolation of data from disparate sources. Acoustic and light detection and ranging radar (LiDAR) is commonly used in conventional surveying above ground level, while single-beam echo sounder (SBES) and multi-beam echo sounder (MBES) are used below water or sea level. Depth values depending on X and Y horizontal coordinates are measured by the above methods. During the post-processing of the elevation profile, the integration of multiple methods requires significant experience. Also, data with different densities must be interpolated and modeled to produce proper resolution and a reliable cross section using different interpolation techniques. In addition, researchers would like to be able to incorporate data acquired through geostatistics, remote sensing (RS), and geographic information systems (GIS) technologies made possible by the development of satellite technologies in recent years. The demand for acquiring rapid and economic spatial information has exceeded the limits of conventional survey methods, driving the interest in new technologies.

Additionally, a challenge of down-scaling spatial information is to identify the coherence between images when using limited high-resolution information to produce a downscaled series of images (Atkinson, 2013). Engineers require a reliable method to distinguish real changes in signal from noise. Researchers have developed complex models to simulate higher spatial resolution images, automatically identifying and locating land cover targets at subpixel scales (Dai et al., 2009). However, engineers often work on lower resolution images to achieve their goals. Finally, the issue of climate change has created great demand for real-time applications that estimate and model areas with complex topography in large-scale 3D environments (Herzfeld et al., 2011; Wang et al., 2012; Rogelis and Werner, 2013). This paper presents an open source, automation interpolation system based on the

Paper submitted 12/04/14; revised 05/10/15; accepted 05/12/15. Author for correspondence: Edward H. Wang (e-mail: edwang313@gmail.com).
[1] Department of Harbor and River Engineering, National Taiwan Ocean University, Keelung, Taiwan, R.O.C.
[2] Department of Civil Engineering and Environmental Informatics, Minghsin University of Science and Technology, Hsinchu, Taiwan, R.O.C.

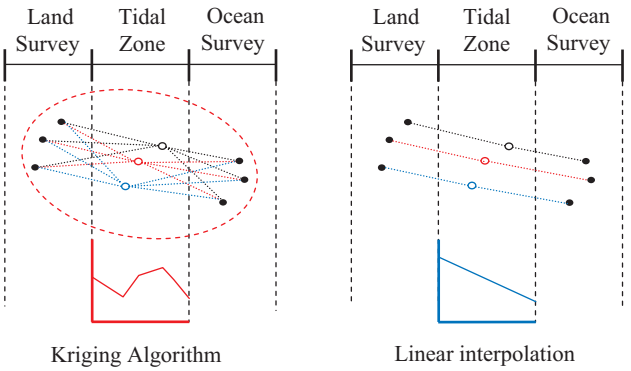

Fig. 1. Comparison between the Kriging method and linear interpolation.

Kriging algorithm using cloud computing on the internet.

Developed by the French mathematician, Georges Matheron in 1970, the Kriging algorithm offers optimal interpolation based on regression against observed z values of surrounding data points, weighted according to spatial covariance values. Although the Kriging method originated from seeking to estimate the most likely distribution of gold ore, based on samples from a few boreholes, it became a general method of statistical interpolation that can be applied within any discipline to sample data from random fields that satisfy the appropriate mathematical assumptions. Competing modeling techniques include inverse distance, local polynomial, minimum curvature, moving average, nearest-neighbor, Delaunay interpolation methods, Polynomial Regression (PR), and Radial Basis Functions (RBF) etc. A number of researchers have concluded that the Kriging Method offers the most satisfactory result overall (Karl, 2010; Aykut et al., 2013). A simple illustration of Kriging approach compared with linear interpolation is shown in Fig. 1. In addition to its mining and natural resources identification applications, Kriging has been widely used in a variety of disciplines, including: agricultural management (Johnson et al., 2012; Adjorloloa and Mutanga, 2013), water resources and hydrogeology (Coskun et al., 2010; Ma et al., 2012; Schilling and Jacobson, 2012), environmental monitoring (Lin et al., 2009; Kumar et al., 2011; Lee et al., 2012), urban planning and real estate appraisal (Emadi et al., 2010; Liu et al., 2013), and quantifying environmental indicators (Shamsudduh et al., 2009; Jun and Ghosh, 2011; Atkinson, 2013). Another important and rapidly growing field of engineering application of Kriging is the interpolation of response variable data from deterministic computer simulations, e.g. finite element method (FEM) simulations.

Ordinary Kriging follows straightforwardly from the model, but small changes in the model function and its parameters can affect the Kriging error variances. The Kriging method can only be advantageous if one thoroughly understands the theory behind it. To enable users to skip the learning curve and ease the applicability of Kriging method, the research team streamlined the automation process by minimizing human error and optimizing all possible alternatives. The Kriging method, combined with other technology, is producing rapid growth of advanced technology with many applications (Liao et al., 2013). The research team took advantage of rapid internet growth to develop a network of interconnected objects called the Internet of Things (IoT) (Ma et al., 2012). This automation-in-processing approach enables end users to integrate scattered field point data and high-resolution remote-sensing images, providing a new basis to map unreachable terrain and allowing its future application in agricultural management, environmental habitat protection, conservation assessment and long-term ecological monitoring in various landscapes on the Earth's surface.

II. MAJOR RESEARCH ACTIVITIES

1. Pilot Study

It is prudent to exhaust the most current technology available today to validate the results of a pilot test. Similar to a study that compared radar tomography (RT) results with those from a radar-sounding profiler using the principles of mass conservation (Morlighem et al., 2012), the research team constructed various variogram models in different directions and grid sizes, followed the ordinary Kriging method using software package EasyKriging 3.0, and then compared the model data with the actual field data obtained from LiDAR and Total Station on a sandy beach in Yen-Liao, Taiwan. Table 1 and Table 2 show the detail specification of the LiDAR LAMS 420i and Total Station LEICA 703 Model used in the pilot study, respectively. As shown in Fig. 2, the size of the red block on the right is 160 m × 80 m. The pilot study also fine-tuned the standard operation procedure, derived coordinate transformation, and identified the minimal precision when applying ordinary Kriging in local roughness on fracture surface topography compared to sequential Gaussian simulation (Hirotaka and Giovanni, 2010). The pilot study confirmed that the Kriging method is an adequate approach in interpolating ground profile within +/- 25 cm marginal accuracy. A maximum 20 m distance between cross sections and no more than 10 m between data points are preferable.

Prior to the pilot study, one must start a lengthy process constructing an adequate data variogram model to obtain meaningful output. In the pilot study an initial aerial topography collected by LiDAR compared with results from topography estimated by Kriging estimation. The results converge well and are agreeable with Gaussian model. Also, the pilot study confirmed the need for the development of a mechanism simplifying the Kriging algorithm. For the number of points and distribution data governs the Kriging estimate substantially.

2. Streamlining the Kriging Algorithm

In the second stage of the research program, instead of adopting commercially available software, the team developed a comprehensive geostatistical methodology that accounts for roughness characteristics in fracture surface topography. The

Table 1. Detail model specification of LiDAR.

Model LMS Z420i	
Distance Range	Up to 1,000 m (80% refection); 350 m + 10 (reflection)
Distance Accuracy	8 mm (single); 4 mm (average)
Light Beam Parameter	0.25 mrad = 0.014°
Built-in Program	Setout/Surveying/Free Station/Area/Tie distance
Speed	11,000 points/sec
Scan Range	0 to 80° in vertical; 0 to 360° horizontal
Scan Resolution	314 in.

Table 2. Detail model specification of total station.

Model LEICA 703	
Angle Measurement	3", 1 mgon
Distance Measurement	3,000 m (with reflector); 2 mm + 2 ppm 170 m (w/o reflector); 3 mm ± 2 ppm
Measuring Time	< 1 sec (with reflector) 3 sec (w/o reflector up to 30 m)
Built-in Program	Setout/Surveying/Free Station/Area/Tie distance
Recording	4,500 measurements and 7,000 fix points RS232 interface for external connection
Magnification	30X
Plummet	Laser: located in alidade, turn with instrument, accuracy ±0.8 mm at 1.5 m

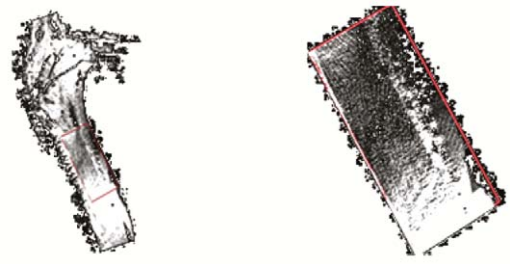

Fig. 2. Scanned Point Cloud of Sandy Beach in the Pilot Study.

proposed approach requires characterizing small-scale fracture surface roughness into numerous "locally defined patterns" that recognize the relative height of a location compared to its surrounding locations. The research team established the Kriging Variogram Data Bank from a massive 20 m grid 1/5,000 DEM library sponsored by the Ministry of Interior of Taiwan. Through minimization of local error variance and reproduction of local roughness characteristics into an objective function of simulated annealing, the fracture surface topography process is improved by cross validation cycling. Research clearly indicated that the function for the spatial covariance, or more widely, of the variogram is crucial for a sound Kriging interpolation. The variogram must be estimated reliably and then modeled with valid mathematical

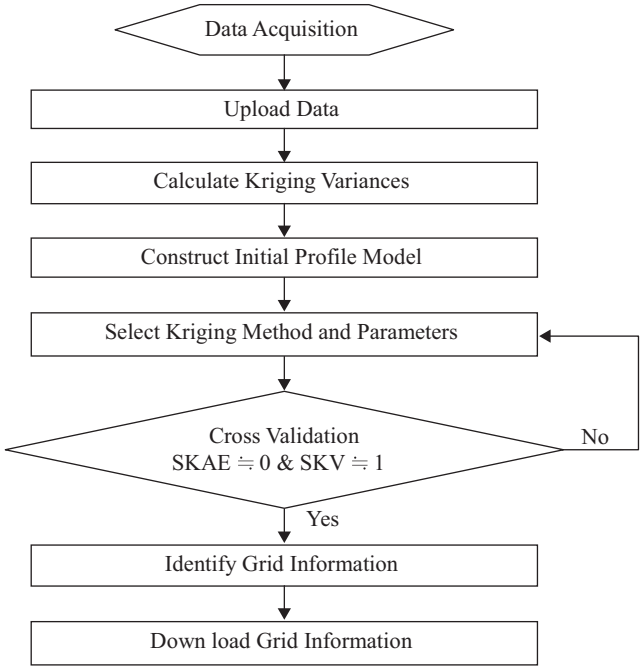

Fig. 3. Flowchart of ordinary data processing.

functions (Oliver and Webster, 2014). The research team streamlined the flow chart of ordinary data processing as shown in Fig. 3.

3. Cross Validation

Researchers conducted cross validation procedures and Monte Carlo simulations to quantify the uncertainty in the resulting map (Arieira et al., 2011). Cross validation showed that accuracy in classification varies with the targeted object type, as a result of sampling density and configuration. A map of uncertainty derived from Monte Carlo simulations revealed significant spatial variation in classification, but this had little impact on the proportion and arrangement of the targeted objects observed. These results suggested that mapping improvement could be achieved by increasing the number of field observations of those objects with a scattered and small patch size distribution; or by including a larger number of digital images as explanatory variables in the model.

The objective of cross validation is to minimize the Standardized Kriging Average Error, SKAE. In other words, the deviation between the projected values and the actual values should be minimized. The formula of Standardized Kriging Average Error is:

$$SKAE = \frac{1}{n}\sum_{i=1}^{n}\left[\frac{Z_i^* - Z_i}{\sigma_{Z_i}}\right] \cong 0 \qquad (1)$$

where n is the number of actual data points, Z_i^* is projected Covariance, Z_i is an actual value, and σ_{Z_i} is the Kriging Variance.

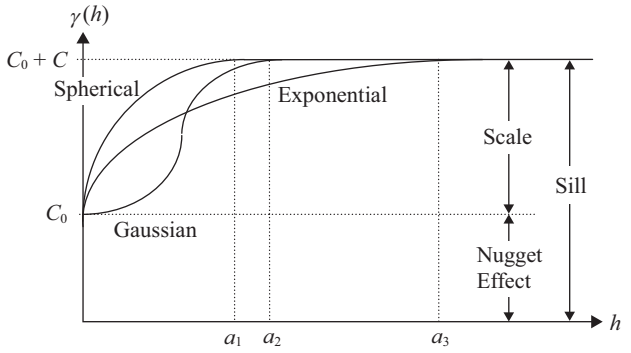

Fig. 4. Models used in the Experimental Variogram.

The second objective of cross validation is to push the Standardized Kriging Variance, SKV, toward unity, indicating consistency between projected values and actual values. The formula of Standardized Kriging Variance, SKV is:

$$SKV = \frac{1}{n}\sum_{i=1}^{n}\left[\frac{(Z_i^* - Z_i)^2}{\sigma_{Z_i}^2}\right] \cong 1 \tag{2}$$

where $\sigma_{Z_i}^2$ is the Kriging Variance Coefficient, is calculated as:

$$\sigma_{z_i}^2 = \mu + \sum_{i=0}^{n}\lambda_i \gamma\left(Z_i^* - Z_i\right) \tag{3}$$

μ is a constant and λ represents weighing factors. $\gamma(h)$ is the Experimental Variogram which incorporates four different models, including Model in Nugget Effect, Spherical, Exponential, and Gaussian Models as shown in Fig. 4. This research program used the Spherical Model where the curve value reaches the constant, Sill. Sill is the combination of the Scale and Nugget Effect, C_0. The model dictates the effect of variations from points within a specific distance range. The formulas of the Spherical Models are:

$$\gamma\left(h\right) = C_0 + C_1\left[1.5\left(\frac{h}{a}\right) - 0.5\left(\frac{h}{a}\right)^3\right], \quad if \quad h < a$$

$$\gamma\left(h\right) = C_0 + C_1, \quad if \quad h > a \tag{4}$$

The cross validation procedure includes the following steps: (a) Construct an initial variogram model and its parameters in accordance with the variogram function obtained from sample data; (b) Remove the first observed value $Z(X_1)$ as unknown; (c) Establish Kriging variance by using the rest of the data observed and estimate the $Z^*(X_1)$ value at point X_1; (d) Reassign the original $Z(X_1)$ value back to the data series. Repeat steps (a) to (d) at all points until all values are estimated. (e) Analyze the original data and estimated values using proper statistics, such as SKV. (f) Justify the adequacy of the model based on previous step; (g) Repeat steps (a) to (f) adjusting parameters or selecting other models until satisfactory results are obtained.

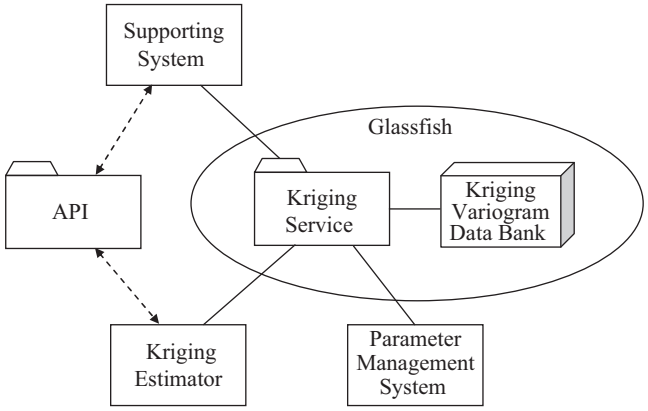

Fig. 5. The Kriging cloud computing framework.

4. User Friendly Cloud Computing System

The overall Kriging cloud computing framework features several key components written in a common server-side programming language, JavaScript on Java 2 Platform Enterprise Edition (J2EE). As shown in Fig. 5, an open-source application server sponsored by the Oracle Corporation called Glassfish hosts two of the main framework components: the Kriging Algorithm Chamber and the Kriging Variogram Data Bank supported by the Google Web Tool (GWT). The Kriging Algorithm Chamber contains formulae and constants of Simple Kriging, Ordinary Kriging and Universal Kriging. The Kriging Variogram Data Bank consists of various local variograms characterized from massive DEMs. The information exchange mechanism adopts JSON-RPC, a lightweight remote procedure call protocol to invoke systems. The application programming interface (API) developed by the research team specifies the details from initiation of a notification to receiving responses from the Kriging Parameter Management System, Kriging Estimator and other associated systems.

III. RESULTS AND ANALYSIS

1. Cloud Computing System

The system is secured at the server of the Ocean Surveying Laboratory, Department of Harbor and River Engineering, National Taiwan Ocean University (http://140.121.145.85/osl-Krige-war). End users may upload a profile data file and assign the targeted grid to start the Kriging Analyzer process. The Kriging Analyzer follows the flowchart shown in Fig. 6 while the Kriging Estimator will process data specified by the API following the flowchart shown in Fig. 7. After data entry, the interactive system allows end users to specify all parameters to start model construction at the targeted area of interest as shown in Fig. 8. A typical output shows the selection of a proper variogram in two directions, x and y by the cloud computing system as shown in Fig. 9. Several sample results

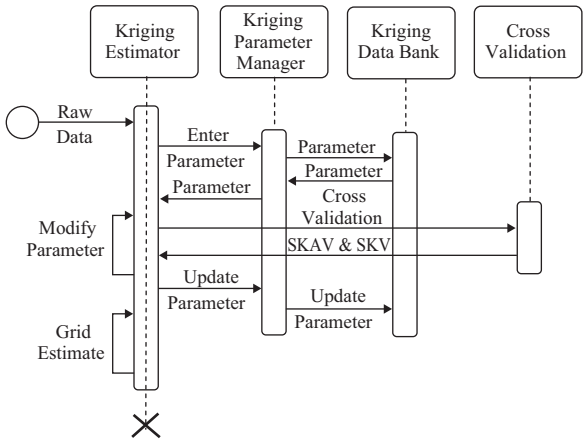

Fig. 6. Flowchart of the Kriging Analyzer.

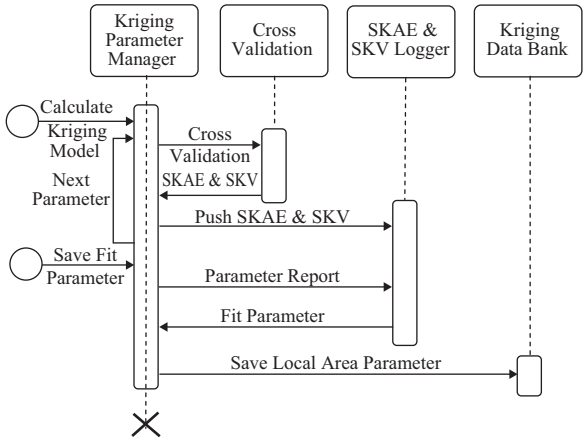

Fig. 7. Flowchart of the Kriging Estimator.

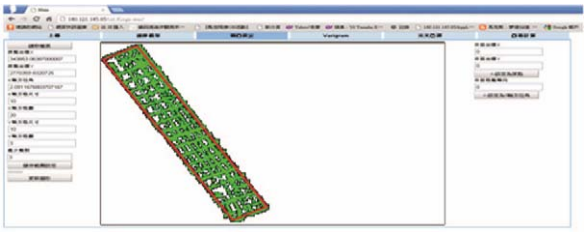

Fig. 8. Defining the area of interest in the Kriging Analyzer.

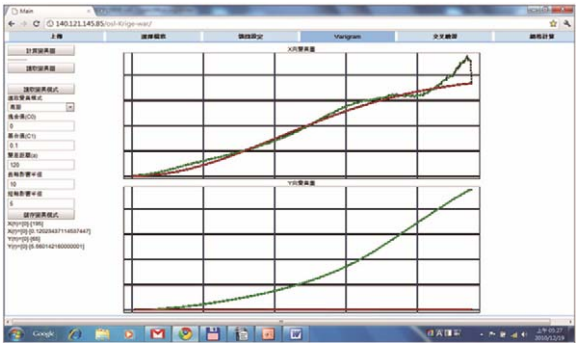

Fig. 9. Selecting a proper variogram in two directions, X and Y.

Table 3. Sample results of Kriging modeling.

Photo Series No.	Longitude	Latitude	Key Axis Isotropy	Model Parameters		
				a	C_0	C_1
94171005	120.383	22.49102	45	30	0.04	0.25
94171006	120.3831	22.49824	0	40	0	0.23
94171028	120.4578	22.44451	0	40	0	0.29
94171029	120.4582	22.44668	57	50	0.008	0.29
94182051	120.2583	22.62216	0	30	0.009	0.09
94182061	120.2829	22.5894	60	40	0.009	0.09
94182072	120.2959	22.57321	32	60	0.009	0.11
94182083	120.3081	22.54526	45	60	0.004	0.13
94182094	120.3395	22.52318	45	60	0.009	0.05
94183010	120.2412	22.74815	0	30	0.004	0.27
94183020	120.2534	22.7231	0	40	0	0.27
94183030	120.2534	22.69511	49	50	0.001	0.23
94183040	120.2499	22.65626	0	60	0.001	0.29
94183050	120.2507	22.64669	0	40	0.001	0.29
94184006	120.1361	22.99812	45	30	0.001	0.29
94184017	120.1581	22.96428	0	30	0.003	0.29
94184027	120.1734	22.94775	0	30	0.001	0.27
94184037	120.1738	22.92084	0	30	0.003	0.29
94184047	120.1798	22.89812	0	40	0.004	0.27
94184058	120.1904	22.87325	10	50	0.002	0.29
94184068	120.1927	22.84815	0	30	0.009	0.09
94184078	120.1898	22.814	0	40	0.001	0.27
94184089	120.2176	22.7968	26	60	0.004	0.15
94184099	120.229	22.7732	0	40	0.009	0.25
94193013	120.0769	23.19861	0	40	0.001	0.25
94193023	120.0648	23.17416	0	40	0.001	0.25
94193033	120.0581	23.15696	0	40	0	0.23
94193042	120.0572	23.14522	0	40	0.003	0.27
94193043	120.0581	23.14811	0	30	0.002	0.13
94193052	120.0349	23.09885	0	40	0.009	0.27
94193062	120.0332	23.0853	0	40	0	0.27
94193072	120.0374	23.07105	0	30	0	0.19
94193082	120.0581	23.04788	0	50	0.002	0.03
94193083	120.0581	23.0477	0	60	0	0.29
94193094	120.108	23.02307	90	40	0.001	0.27
94193095	120.1082	23.02325	0	40	0.002	0.29

Note: Key Axis Isotropy defines the covariance in length and angle between two data.

of Kriging Modeling followed by cross validation are listed in Table 3. Currently, the overall input-output interfaces are in the Chinese language. An English user manual is in development to prepare for conversion to an English version interface.

2. Future Development of the Study

As indicated by Hession and Moore, Kriging and spline-

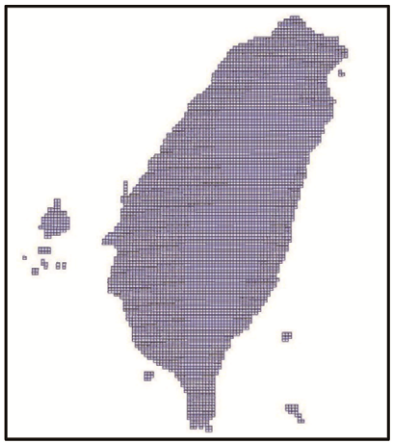

Fig. 10. Divisions of aerial photos of Taiwan.

based studies often focus on providing improved predictions rather than understanding. (Hession and Moore, 2011) It is recommendable to all users to familiarize with the bases of Kriging algorithm. This research developed the Kriging cloud computing framework and facilitates a self-learning tool by integrating multidisciplinary technology. A pilot study at a Yen-Liao sandy beach laid the fundamental foundation of the system. More detailed iterations and complicated modeling of the majority of rocky and hilly areas on the east coast of Taiwan strengthened the knowledge gained and showed the need for further research. Taiwan is an island with a length of four hundred kilometers and a width of one hundred kilometers. The total area is 36,000 km^2. Two-thirds of Taiwan's landmass is covered by the Central Mountain Range where its peak, Yu Shan, is 3,952 meters in height. Taiwan's eastern two-thirds terrain is mostly rugged mountains; flat to gently rolling plains cover the west. The mountainous area above 1,000 meters occupies 32% of the island's area, hills and plateaus between 100 meters and 1,000 meters cover 31%, and the rest is plains with elevation below 100 meters. The research team continues the effort in an attempt to cover every possible landscape around the island as shown in Fig. 10. Since natural disasters usually result in widespread destruction of property or loss of life, and more than 75 percent of Taiwan is urbanized, hazard prevention and emergency response is imperative today. Once completed, the Kriging cloud computing framework provides a comprehensive data process engine applicable to urban planning, disaster mitigation, and long term earth surface observation, even in unreachable terrain. Finally, as the global warming continues to melt Antarctica's ice and threatening the oceanic and near shore wildlife, the research may further develop an instantaneous, interactive tool for marine time research on the impact assessment of climate change.

IV. CONLCUSION

There have been several reliability and cost issues related to the interpolation of topography surveyed by satellite images with differing resolution or acoustic and LiDAR from human operation. Fusion of multi-technologies and obstacles in remote areas frequently raise concerns about the proper training and personal safety of field investigators. To produce thorough ground profiles in a conventional manner, surveying crews sometimes must risk their lives to physically penetrate difficult areas to conduct surveying through direct contact. Moreover, timing is crucial and the data collected must be thorough for the decision maker to make a timely, comprehensive analysis. It is desirable to measure the overall spatial information in a short period of time by adopting functions validated through a rich data bank and taking advantage of the speed of the internet. The research program shortened the operational path, streamlined the process, and pushed the envelope of what cloud computing can offer. This paper reports the development of a cloud computing framework based on the Kriging algorithm and produced an example of the automatic interpolation of near-shore sea bed and beach profile. This framework should be widely applicable to an array of remote locations including deserts, swamps, dense forests, and rugged mountains or even aiding in the exploration of other planets in the universe.

ACKOWNLEDGMENTS

This work was supported by the National Science Foundation in Taiwan, Grant No. NSC100-2221-E-019-010.The authors would like to thank all colleagues and students who contributed to this study.

REFERENCES

Adjorloloa, C. and O. Mutanga (2013). Integrating remote sensing and geostatistics to estimate woody vegetation in an African savanna. Journal of Spatial Science 58(2), 305-322.

Arieira, J., D. Karssenberg, S. M. Jong, E. A. Addink, E. G. Couto, C. N. Cunha and J. O. Skøien (2011). Integrating field sampling, geostatistics and remote sensing to map wetland vegetation in the Pantanal, Brazil. Biogeosciences 8, 667-686.

Atkinson, P. M. (2013). Downscaling in remote sensing. International Journal of Applied Earth Observation and Geoinformation 22, 106-114. http://dx.doi.org/10.1016/j.jag.2012.04.012

Aykut, N. O., B. Akpınar and O. Aydın (2013). Hydrographic data modeling methods for determining precise seafloor topography. Computational Geosciences 17(4), 661-669.

Coskun, H. G., U. Alganci, E. Eris, N. Agıralioglu, H. K. Cigizoglu, L. Yilmaz and Z. F. Toprak (2010). Remote sensing and GIS innovation with hydrologic modeling for hydroelectric power plant (HPP) in poorly gauged basins. Water Resources Management 24(14), 3757-3772.

Dai, X., Z. Guo, L. Zhang and X. Xu (2009). Subpixel mapping on remote sensing imagery using a prediction model combining wavelet transform and radial basis function neural network. Journal of Applied Remote Sensing 3(1). DOI:10.1117/1.3277121.

Emadi, M., M. Baghernejad, M. Pakparvar and S. A. Kowsar (2010). An approach for land suitability evaluation using geostatistics, remote sensing, and geographic information system in arid and semiarid ecosystems. Environmental Monitoring and Assessment 164(1-4), 501-511.

Herzfeld, U. C., B. F. Wallin, C. J. Leuschen and J. Plummer (2011). An algorithm for generalizing topography to grids while preserving subscale

morphologic characteristics—creating a glacier bed DEM for Jakobshavn trough as low-resolution input for dynamic ice-sheet models. Computers & Geosciences 37(11), 1793-1801.

Hession, S. L. and N. Moore (2011). A spatial regression analysis of the influence of topography on monthly rainfall in East Africa. International Journal of Climatology 31(10), 1440-1456.

Hirotaka S. and G. Giovanni (2010). Geostatistical downscaling of fracture surface topography accounting for local roughness. Acta Geotechnica 5(2), 127-138.

Johnson, B., R. Tateishi and T. Kobayashi (2012). Remote sensing of fractional green vegetation cover using spatially-interpolated end members. Remote Sens 4(9), 2619-2634.

Jun, G. and J. Ghosh (2011). Spatially adaptive classification of land cover with remote sensing data. IEEE Transactions on Geosciences and Remote Sensing 49(7), 2662-2673.

Karl, J. W. (2010). Spatial predictions of cover attributes of rangeland ecosystems using regression Kriging and remote sensing. Rangeland Ecology & Management 63(3), 335-349.

Kumar, N., A. D. Chu, A. D. Foster, T. Peters and R. Willis (2011). Satellite remote sensing for developing time and space resolved estimates of ambient particulate in Cleveland, OH. Aerosol Science and Technology 45(9), 1090-1108.

Lee, S. J., M. L. Serre, A. Donkelaar, R. V. Martin, R. T. Burnett and M. Jerrett (2012). Comparison of geostatistical interpolation and remote sensing techniques for estimating long-term exposure to ambient PM2.5 concentrations across the continental United States. Environ Health Perspectives 120(12), 1127-1732.

Liao, K., S. Xu, J. Wu and Q. Zhu (2013). Spatial estimation of surface soil texture using remote sensing data. Soil Science and Plant Nutrition 59(4), 488-500.

Lin, Y. P., H. J. Chu, C. L. Wang, H. H. Yu and Y. C. Wang (2009). Remote sensing data with the conditional Latin Hypercube Sampling and geostatistical approach to delineate landscape changes induced by large chronological physical disturbances. Sensors 9(1), 148-174.

Liu, Q., Y. Pan, B. Chen, S. Li and A. Guo (2013). Analysis on the relationship and its dynamics between rural settlements and linear features using GIS and RS. Intelligent Automation & Soft Computing 18(8), 1053-1062.

Ma, D., Q. Ding, Z. Li, D. Li and Y. Wei (2012). Prototype of an aquacultural information system based on Internet of Things E-Nose. Intelligent Automation & Soft Computing 18(5), 569-579.

Morlighem, M., E. Rignot, J. Mouginot, X. Wu, H. Seroussi, E. Larour and J. Paden (2012). High-resolution bed topography mapping of Russell Glacier, Greenland, inferred from Operation Ice Bridge data. Journal of Glaciology 59(218), 1015-1023.

Oliver, M. A. and R. Webster (2014). A tutorial guide to geostatistics: Computing and modeling variograms and Kriging 113, 56-69.

Rogelis, M. C. and M. G. F. Werner (2013). Spatial interpolation for real-time rainfall field estimation in areas with complex topography. Journal of Hydrometeor 14, 85-104.

Schilling, K. E. and P. Jacobson (2012). Spatial relations of topography, lithology and water quality in a large river floodplain. River Research and Applications 28(9), 1417-1427.

Shamsudduha, M., L. J. Marzen, A. Uddin, M. K. Lee and J. A. Saunders (2009). Spatial relationship of groundwater arsenic distribution with regional topography and water-table fluctuations in the shallow aquifers in Bangladesh. Environmental Geology 57(7), 1521-1535.

Wang, C., T. R. Wan and I. J. Palmer (2012). Automatic reconstruction of 3D environment using real terrain data and satellite images. Intelligent Automation & Soft Computing 18(1), 49-63.